

Supporting Information

**Dimerization Induced Deprotonation of Water on RuO<sub>2</sub>(110)**

Rentao Mu,<sup>‡, a, c</sup> David C. Cantu,<sup>‡, a, c</sup> Xiao Lin,<sup>‡, a, c</sup> Vassiliki-Alexandra Glezakou,<sup>a, c</sup> Zhitao Wang,<sup>b, c</sup> Igor Lyubinetsky,<sup>b, c</sup> Roger Rousseau,<sup>\*, a, c</sup> and Zdenek Dohnálek<sup>\*, a, c</sup>

<sup>a</sup> *Fundamental and Computational Sciences Directorate,* <sup>b</sup> *Environmental Molecular Sciences Laboratory,* <sup>c</sup> *Institute for Integrated Catalysis, Pacific Northwest National Laboratory, P.O. Box 999, Richland, Washington 99352, United States*

## 1. STM Images of Clean Stoichiometric RuO<sub>2</sub>(110)

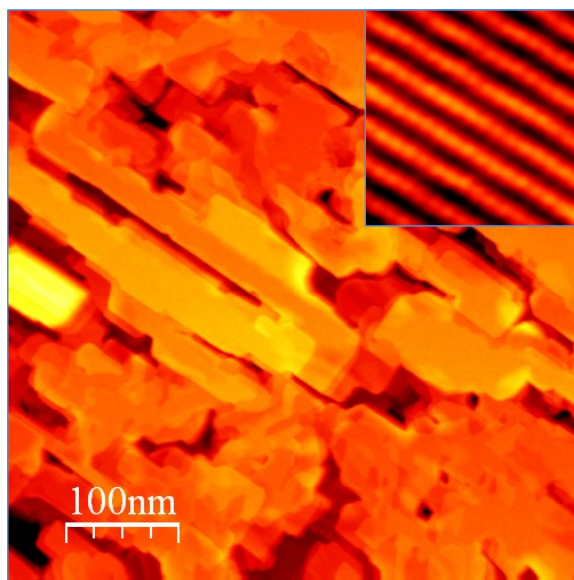


**Figure S1:** A large scale STM image of stoichiometric RuO<sub>2</sub>(110) thin film grown on Ru(0001) substrate. Inset: A high-magnification image ( $5 \times 5 \text{ nm}^2$ ) illustrating surface structure composed of the rows of bright bridge-bonded oxygen ( $\text{O}_b$ ) and dark five-fold-coordinated Ru ( $\text{Ru}_{\text{cus}}$ ) atoms.

## 2. Computed Properties of RuO<sub>2</sub>(110)

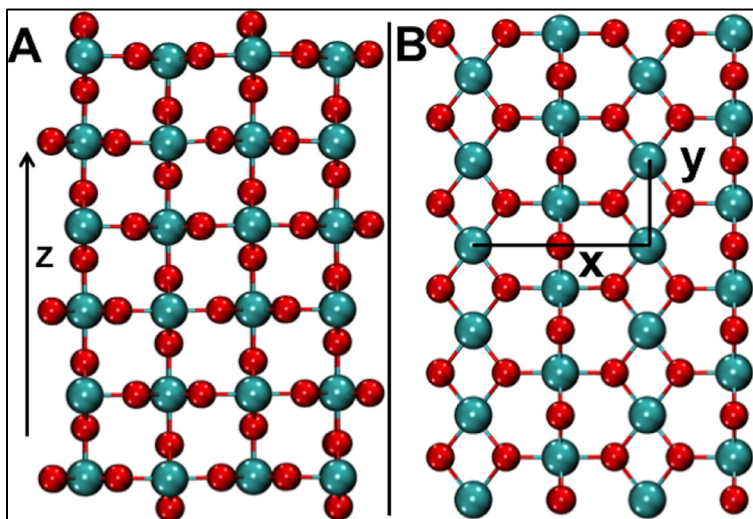


**Figure S2:** A: Side view of the six-layer thick RuO<sub>2</sub> slab. B: RuO<sub>2</sub>(110) surface viewed from above. Red: oxygen; blue: ruthenium.

RuO <sub>2</sub> Surface	This work	Ref. 1	Ref. 2
<b>Surface Dimension x (Å)</b>	6.41	6.38	
<b>Surface Dimension y (Å)</b>	3.13	3.11	
<b>Work Function (eV)</b>	5.6	5.9	5.8

**Table S1:** Computed Properties of RuO<sub>2</sub>(110)

## References

- (1) Kim, Y. D.; Seitsonen, A. P.; Wendt, S.; Wang, J.; Fan, C.; Jacobi, K.; Over, H.; Ertl, G., Characterization of Various Oxygen Species on an Oxide Surface: RuO<sub>2</sub>(110). *J. Phys. Chem. B* **2001**, *105*, 3752-3758.
- (2) Bottcher, A.; Niehus, H., Oxygen Adsorbed on Oxidized Ru(0001). *Phys. Rev. B* **1999**, *60*, 14396-14404.

### 3. STM Images Illustrating Dimerization of Water Molecules

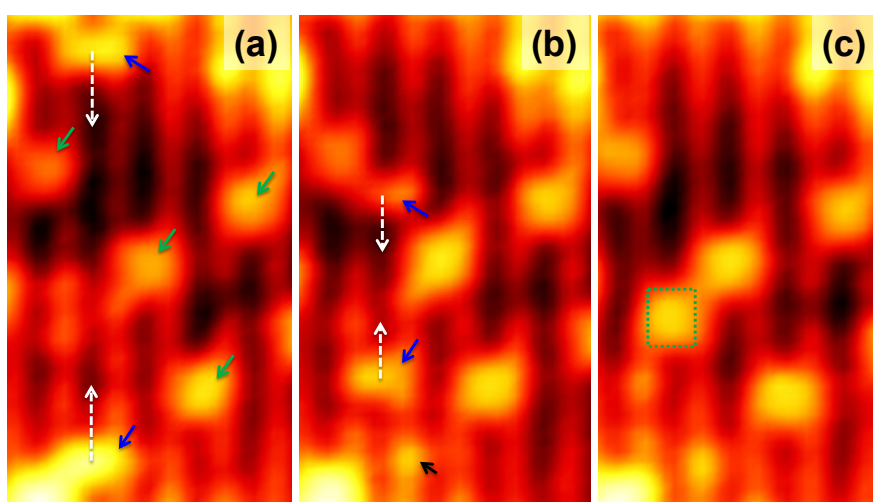


**Figure S3:** A time-lapse sequence of high-magnification STM images ( $4 \times 7 \text{ nm}^2$ ) obtained after  $\text{H}_2\text{O}$  dose on  $\text{RuO}_2(110)$  at 238 K. (b) = (a) + 577 sec, (c) = (b) + 193 s. White dashed arrows illustrate the direction of water monomer diffusion and water dimer formation (green rectangle) in (c). Blue, green and black solid arrows mark water monomers, dimers, and bridging hydroxyl species, respectively.

#### 4. Water Dimer Deprotonation

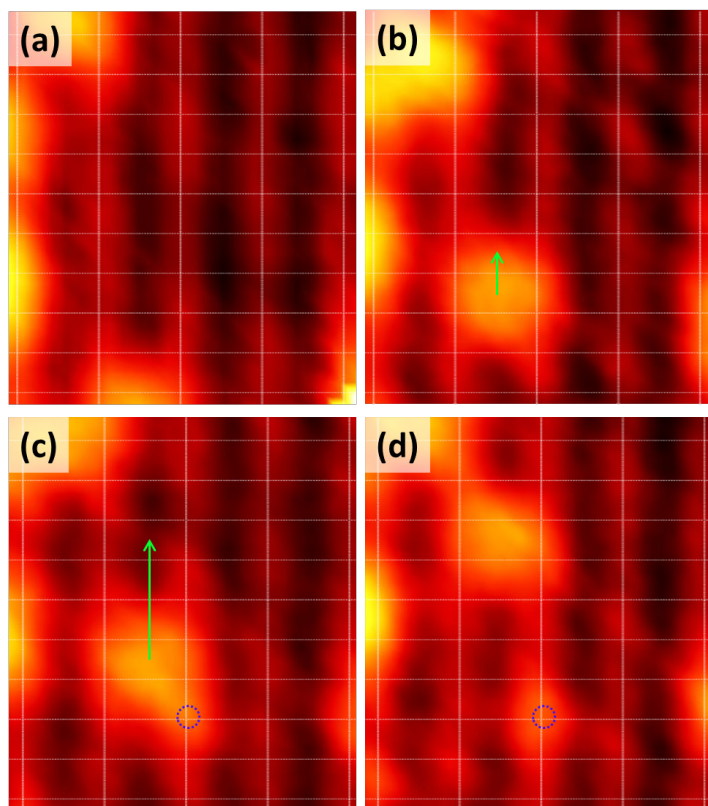


**Figure S4:** Sequence of STM images ( $3.2 \times 3.6 \text{ nm}^2$ ) illustrating the deprotonation of water dimer at 295 K. (b) = (a) + 427 s, (c) = (b) + 256 s, (d) = (c) + 128 s. Green arrows in (b) and (c) illustrate the diffusion of  $\text{H}_3\text{O}_2$  feature formed by  $(\text{H}_2\text{O})_2$  dissociation. Blue circles in (c) and (d) indicate the  $\text{HO}_b$  species formed as a result of  $(\text{H}_2\text{O})_2$  dissociation. The positions of  $\text{O}_b$  atoms in (a-d) are marked with white lines.

## 5. Dumbbell Structure of $\text{HO}_t\cdots\text{H}_2\text{O}$ Pair

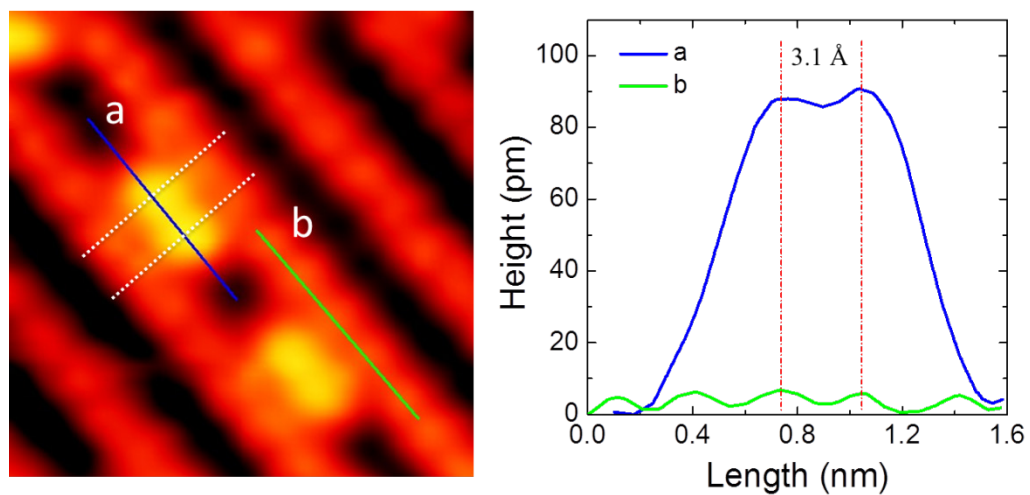


**Figure S5:** Left: High resolution STM image ( $3 \times 3 \text{ nm}^2$ ,  $-0.9 \text{ V}$ ,  $1 \text{ nA}$ ) of  $\text{H}_3\text{O}_2$  species on  $s\text{-RuO}_2(110)$ , illustrating fast proton transfer between two sides of the  $\text{HO}_t\cdots\text{H}_2\text{O}$  pair. Right: Line profiles along the  $\text{Ru}_{\text{cus}}$  row (green: bare surface, blue:  $\text{H}_3\text{O}_2$ ).

## 6. Comparison of Water Energetics on RuO<sub>2</sub>(110) at Different Levels of Theory

RuO <sub>2</sub> (110)	Adsorption	Deprotonation	
	$\Delta E$ (eV/water)	E <sub>BARRIER</sub> (eV)	$\Delta E$ (eV)
<b>Water Monomer</b>			
DFT	-1.15	0.22	-0.02
DFT + D3	-1.36	0.22	0.00
DFT + D3 + ZPE	-1.43	0.03	-0.02
<b>Water Dimer</b>			
DFT	-1.10	0.06	-0.30
DFT + D3	-1.24	0.06	-0.44
DFT + D3 + ZPE	-1.25	No barrier	-0.27

**Table S2:** Water monomer and dimer on RuO<sub>2</sub>(110) adsorption and dissociation (deprotonation) energies with and without D3 and ZPE corrections

RuO <sub>2</sub> (110)	Diffusion Barrier, E <sub>BARRIER</sub> (eV)			
	Water Monomer	Water Dimer	H <sub>3</sub> O <sub>2</sub> with neighboring HO <sub>b</sub>	H <sub>3</sub> O <sub>2</sub> with separated HO <sub>b</sub>
DFT	0.65	0.50	0.65	0.75
DFT + D3	0.65	0.50	0.65	0.75
DFT + D3 + ZPE	0.58	0.45	0.61	0.67

**Table S3:** Water monomer and dimer on RuO<sub>2</sub>(110) diffusion energies with and without D3 and ZPE corrections

## 7. Comparing the Acid/Base Properties of RuO<sub>2</sub> and TiO<sub>2</sub>

Water behavior on both RuO<sub>2</sub>(110) and TiO<sub>2</sub>(110) can be further understood in terms of their acid-base properties. The ratio of our calculated binding energies of water dimers on RuO<sub>2</sub>(110) over water dimers on TiO<sub>2</sub>(110) is 1.28, close to the experimental ratio of 1.3 (See Tables S2 and S4). The stronger water binding on RuO<sub>2</sub> implies a stronger water-metal contact (Lewis acidity), which should, by inductive effects, lead to weaker O-H bonds and therefore a higher Brønsted acidity for the bound waters. To quantify this we consider a hypothetical water adsorption configuration where hydrogen-bonding contacts with the O<sub>b</sub> sites are minimized (see Figure S6). The adsorption energy increases by 0.2 and 0.1 eV for RuO<sub>2</sub> and TiO<sub>2</sub> respectively; hence the overall trend in Lewis acidity (as reflected by the binding energy of the global minimum) is preserved. The impact this has upon the water monomer O-H bond strength (via electrostatic induction) can be measured by the computed red shift in OH frequency, which is found to be 140 and 90 cm<sup>-1</sup> for water on RuO<sub>2</sub>(110) and TiO<sub>2</sub>(110) respectively, indicating that water bound to the Ru site is more acidic than when bound to the Ti site. As a result on the, TiO<sub>2</sub>(110) surface (Table S4) the deprotonated water state is practically isoenergetic (0.03 eV lower) with the molecular water state for the monomer and dimer (0.10 eV lower), but such is not the case on RuO<sub>2</sub>(110). However the deprotonation barriers of water on the TiO<sub>2</sub>(110) surface are considerably higher than on the RuO<sub>2</sub>(110) surface being 0.23 eV for the water monomer and 0.16 eV for the dimer. Consistent with lower adsorption energies due to weaker metal-water interactions, our calculated individual diffusion event barriers for water are lower on the TiO<sub>2</sub>(110) surface than on the RuO<sub>2</sub>(110) surface being 0.35 eV for the monomer and 0.22 eV for the dimer, supporting the role of ruthenium as a stronger Lewis acid.

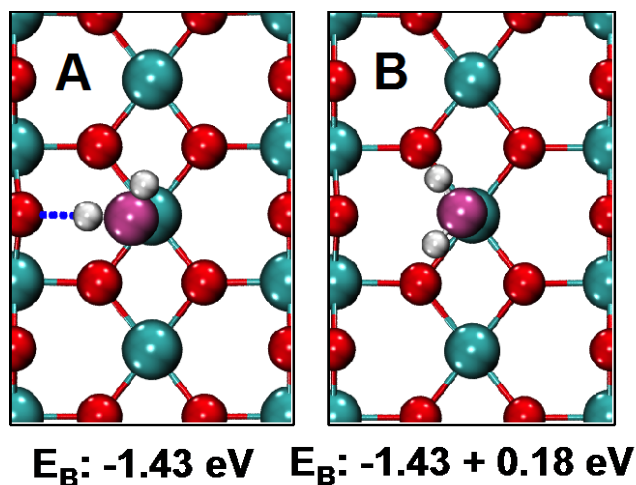


**Figure S6:** Water monomer bound to RuO<sub>2</sub>(110) in (A) the preferred conformation with a hydrogen bond with neighboring O<sub>b</sub>, and (B) without the hydrogen bond. Red: oxygen; pink: oxygen in H<sub>2</sub>O; blue: ruthenium; white: hydrogen.



TiO <sub>2</sub>	Adsorption	Deprotonation	
	$\Delta E$ (eV/water)	$E_{\text{BARRIER}}$ (eV)	$\Delta E$ (eV)
<b>Water Monomer</b>			
DFT	-0.96	0.40	0.02
DFT + D3	-0.91	0.40	0.03
DFT + D3 + ZPE	-0.92	0.23	-0.03
<b>Water Dimer</b>			
DFT	-0.87	0.32	-0.07
DFT + D3	-0.97	0.32	-0.05
DFT + D3 + ZPE	-0.97	0.16	-0.10

**Table S4:** Water monomer and dimer on TiO<sub>2</sub>(110) adsorption, dissociation (deprotonation), and diffusion energies with and without D3 and ZPE corrections.

TiO <sub>2</sub> (110)	Diffusion Barrier, $E_{\text{BARRIER}}$ (eV)			
	Water Monomer	Water Dimer	H <sub>3</sub> O <sub>2</sub> with neighboring HO <sub>b</sub>	H <sub>3</sub> O <sub>2</sub> with separated HO <sub>b</sub>
DFT	0.38	0.32	0.20	0.18
DFT + D3	0.39	0.31	0.19	0.19
DFT + D3 + ZPE	0.35	0.22	0.14	0.12

**Table S5:** Water monomer and dimer on TiO<sub>2</sub>(110) diffusion energies with and without D3 and ZPE corrections

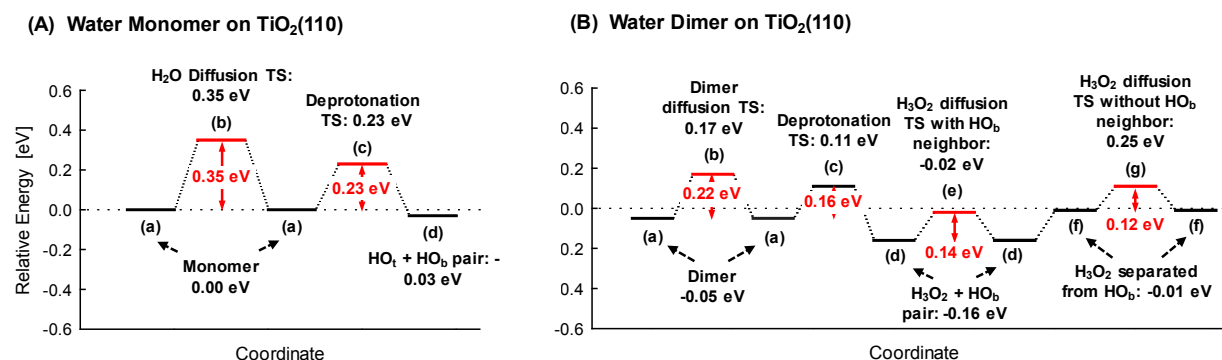


**Figure S7:** Computed potential energy landscape for deprotonation and diffusion of water monomer (A) and dimer (B) on Ti<sub>5c</sub> sites of TiO<sub>2</sub>(110). All energies are calculated using DFT+D3 and corrected for ZPE, using water monomer adsorption as a reference state. Lower values correspond to higher thermodynamic stability.